

ESCAPE OF IONIZING PHOTONS FROM DWARF GALAXIES AT HIGH REDSHIFT

TAYSUN KIMM & RENYUE CEN (PRINCETON)

Kimm & Cen (2014, ApJ, 788, 121)

Introduction

Gunn & Peterson (GP, 1965) predicted that Ly α absorption would give rise to a sudden drop of continuum flux at wavelengths shorter than 1216Å if a tiny amount of neutral hydrogen is present along the line of sight. The dramatic clearing of the Gunn-Peterson trough from the observation of quasars at $z \sim 6$ demonstrates that hydrogen in the Universe is highly ionized at $z < 6$. Yet, the detailed processes on how reionization has occurred remains unclear. It appears that dwarf galaxies are the most plausible source of the ionizing photons, but the major uncertainty in the dwarf galaxy-driven reionization picture is the escape fraction of ionizing photons. In this work, we compute the escape fraction from high-resolution cosmological radiation hydrodynamics simulations with physically based supernova feedback model and runaway OB stars to better understand the reionization history of the Universe.

Cosmological Radiation Hydrodynamics Simulation

Code: RAMSES-RT (Teyssier et al. 2002; Rosdahl et al. 2013)

- Grid-based code with adaptive mesh refinement (moment-based radiation hydrodynamics)

Zoomed-in region: 3.8x4.8x9.6 Mpc³ (out of the total (25Mpc/h)³)

Physical ingredients: metallicity-dependent radiative cooling, stochastic star formation ($n_{\text{H,thres}}=100 \text{ cm}^{-3}$), self-consistent UV heating (HII, HeII, HeIII photons)

New ingredients: Physically based **mechanical supernova feedback**, runaway stars

SUMMARY OF COSMOLOGICAL SIMULATIONS

Model	SNI	RT	Run-aways	Δx_{min} [pc]	$m_{\text{star,min}}$ [M_{\odot}]	m_{dm} [$10^5 M_{\odot}$]
FR	✓	✓	-	4.2	49	1.6
FRU	✓	✓	✓	4.2	49	1.6

A First Self-consistent Feedback Model of Supernova explosions

Energy-based feedback from SN explosions is known to suffer from the artificial radiative cooling if the cooling length is under-resolved. In this case, a *physically correct way would be to deposit the maximum expected momentum*, as at the end of the cooling phase, to the surrounding cells. However, conventional kinetic feedback schemes, based on SN ejecta, impart momentum that is too small by a factor of about ten compared to the terminal momentum.

We have implemented a **new mechanical feedback scheme that can approximate the Sedov solutions at all (from the free expansion to snowplow) phases** by evaluating the amount of mass swept up along each solid angle (or cell). Our new physical scheme produces approximately the correct terminal momentum independent of numerical resolution (Figure 1, left).

$$\Delta p = \begin{cases} \sqrt{2\chi(\Omega)M_{\text{ej}}f_e E_{\text{SN}} \times \frac{\Delta\Omega}{4\pi}} & [\chi(\Omega) \leq \chi_{\text{tr}}(\Omega)] \quad (\text{free + adiabatic phase}) \\ p_{\text{SN}}(E_{\text{SN}}, n_{\text{H}}, Z) \times \frac{\Delta\Omega}{4\pi} & [\chi(\Omega) > \chi_{\text{tr}}(\Omega)] \quad (\text{snowplow phase}) \end{cases}$$

$\chi \equiv \Delta M_{\text{shell}}(\Omega)/\Delta M_{\text{ej}}(\Omega)$ (the ratio between the mass swept up and ejecta mass along each solid angle)
 $\chi_{\text{tr}} \approx 87.54 E_{\text{SN}}^{-2/17} n_0^{-4/17} Z^{-0.28}$ (the mass ratio at the transition from the adiabatic to the snowplow phase)
 $p_{\text{SN}}(E, n_{\text{H}}, Z) \approx 3 \times 10^5 \text{ km s}^{-1} M_{\odot} E_{\text{SN}}^{16/17} n_{\text{H}}^{-2/17} f(Z)$ (momentum at the snowplow phase; Thornton et al. 1998)
 $f(Z) \equiv \max(Z/Z_{\odot}, 0.01)^{-0.14}$

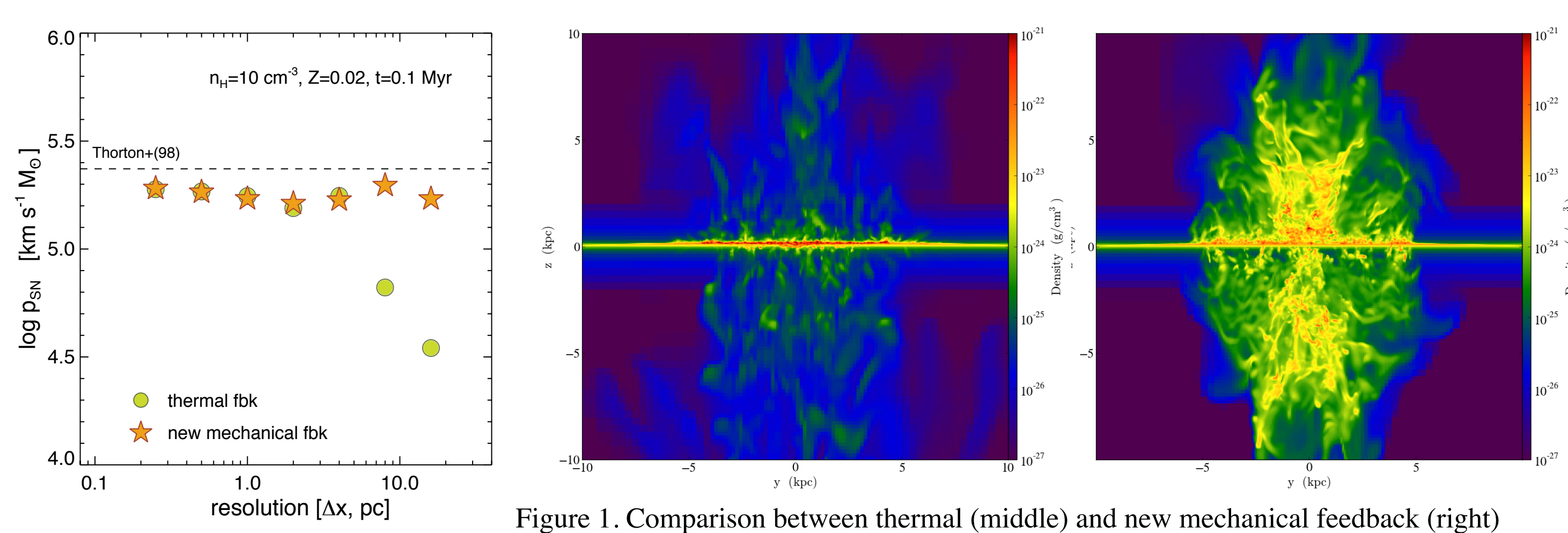


Figure 1. Comparison between thermal (middle) and new mechanical feedback (right)

Results

1. We find that there is a **significant time delay** of about ten million years between the peak of star formation and that of escape fraction, due to the time required for the build-up and subsequent destruction of the star-forming cloud by SN feedback (Figure 1). **This time delay between the peak of star formation and the escape fraction is crucial in predicting the actual escape probability of ionizing photons.** While the instantaneous f_{esc} (solid line) can easily attain $\sim 20\%$, the photon number-weighted mean of the escape fraction (dashed lines) is found to be $\sim 10\%$ (see Figure 3 for the statistical results).

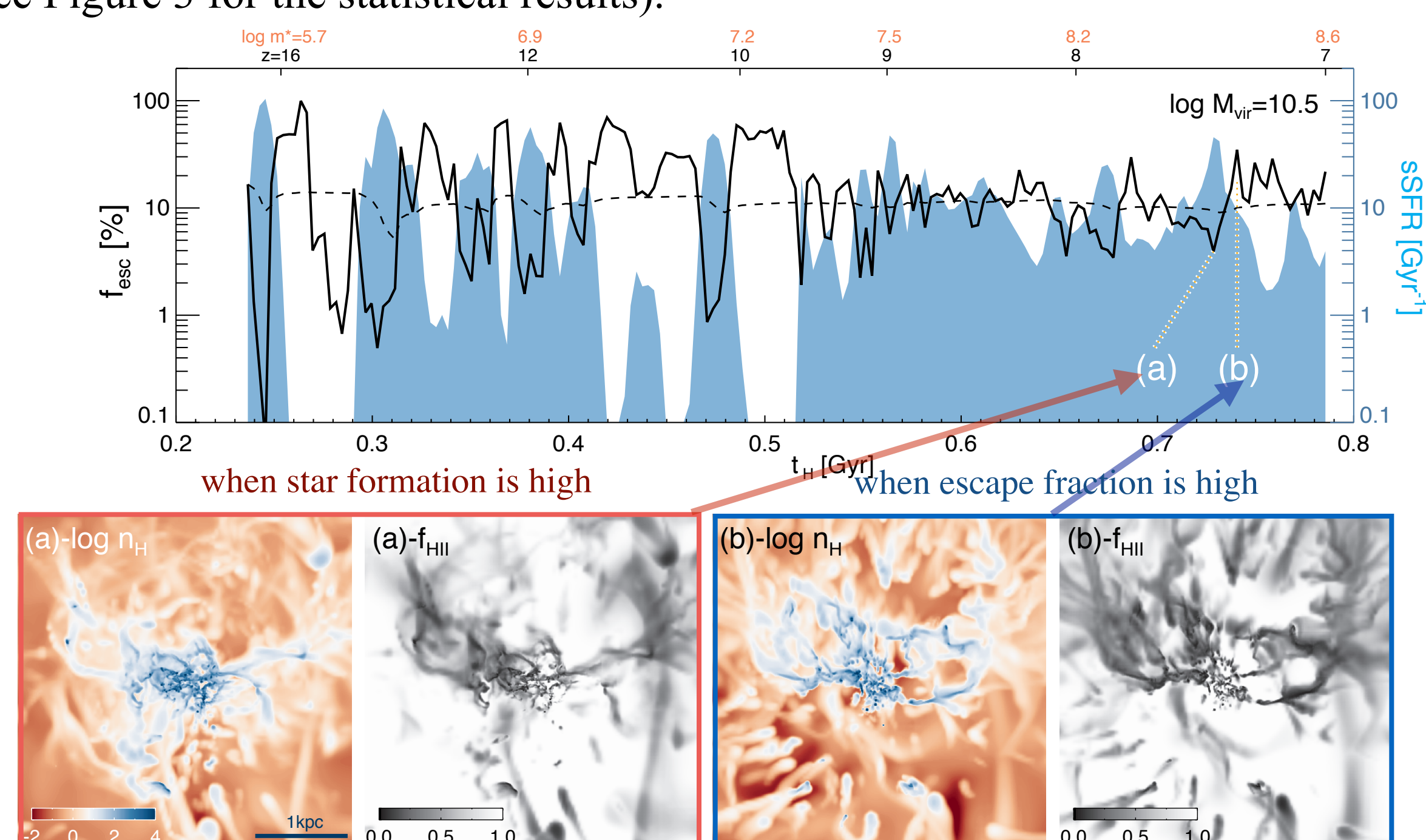


Figure 2. Evolution of the escape fraction (f_{esc}) and specific star formation rate (sSFR) in the most massive halo from the FR run. One can see that there is a delay between the peak in f_{esc} and sSFR due to the delay in the onset of the strong outflow.

2. Although more than 50% of the galaxies reveal the *instantaneous* $f_{\text{esc}} > 10\%$, we find the *photon production-weighted escape fraction to be $\sim 10\text{-}15\%$* , regardless of the halo mass and redshift (Figure 3).

3. **Inclusion of runaway OB stars (FRU run) increases the escape fraction to $\langle f_{\text{esc}} \rangle = 13.8\%$ from 11.4%** (Figure 3). Since the runaway OB stars tend to move to lower density regions, photons from them have a higher chance of escaping. As the runaway OB stars explode in a less dense medium, feedback from SNe becomes more effective, resulting in reduced star formation in halos $M_{\text{vir}} > 10^9 M_{\text{sun}}$, compared with the FR run. Because of the balance between the increase in $\langle f_{\text{esc}} \rangle$ and the decrease in star formation, the total number of ionizing photons escaped by $z = 7$ is found to be comparable in the two run.

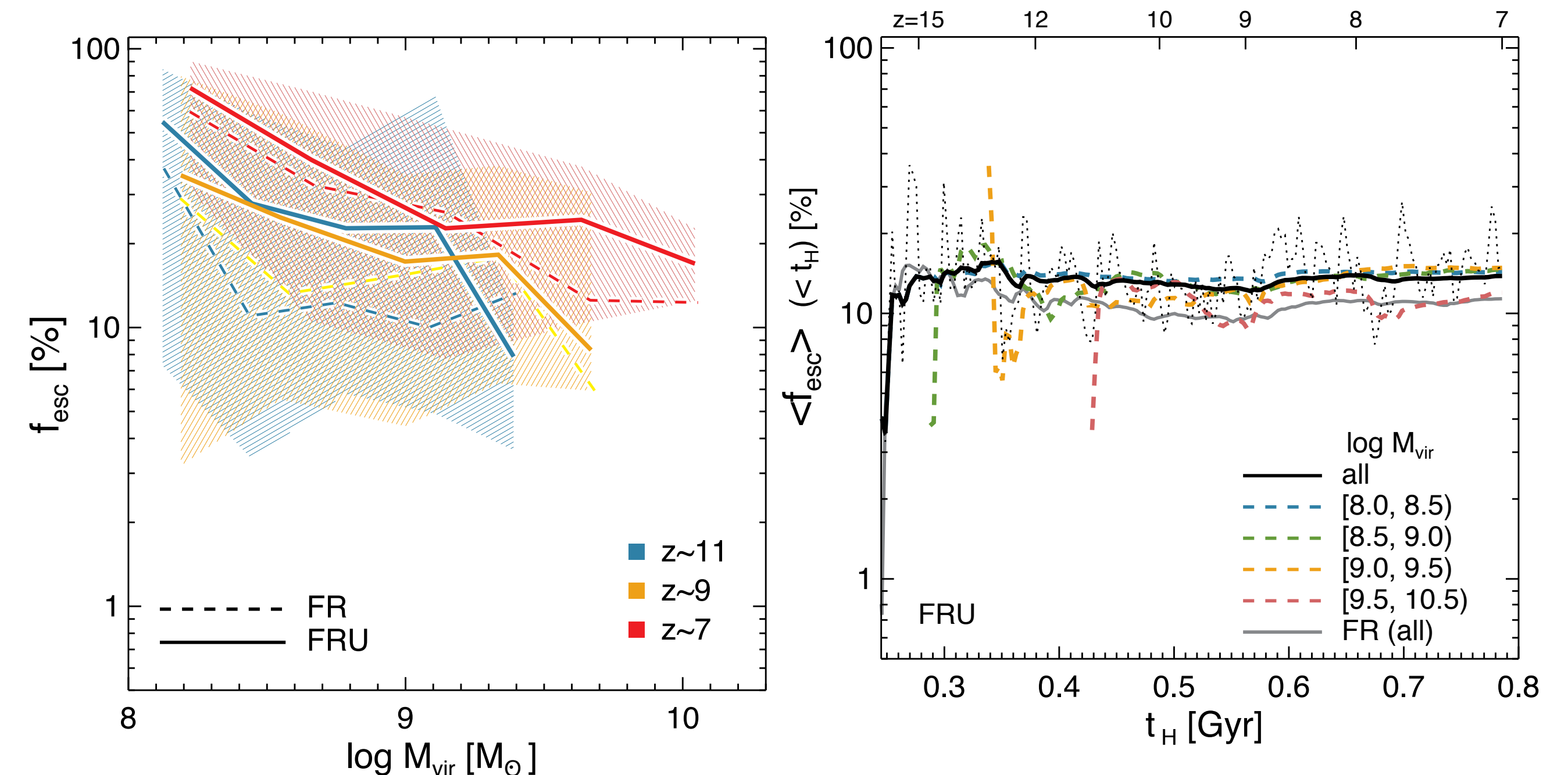


Figure 3. **Left:** Escape fraction measured at the virial radius at three different redshifts from the FR (dashed) and FRU run (solid lines). **Right:** Photon production rate-weighted escape fraction averaged over the age of the universe (t_{H}) in the FR run. We also display the photon rate-averaged escape fraction of the whole sample at each snapshot ($\langle f_{\text{esc}} \rangle(t)$) (black dotted line), as opposed to the time-averaged quantities (solid and dashed lines).

4. **A sufficient amount of photons escape from the dark matter halos with $M_{\text{vir}} > 10^8 M_{\text{sun}}$ to keep the universe ionized at $z < 9$.** The simulated UV luminosity function with a faint end slope of -1.9 is consistent with observations (e.g. McLure et al. 2013).

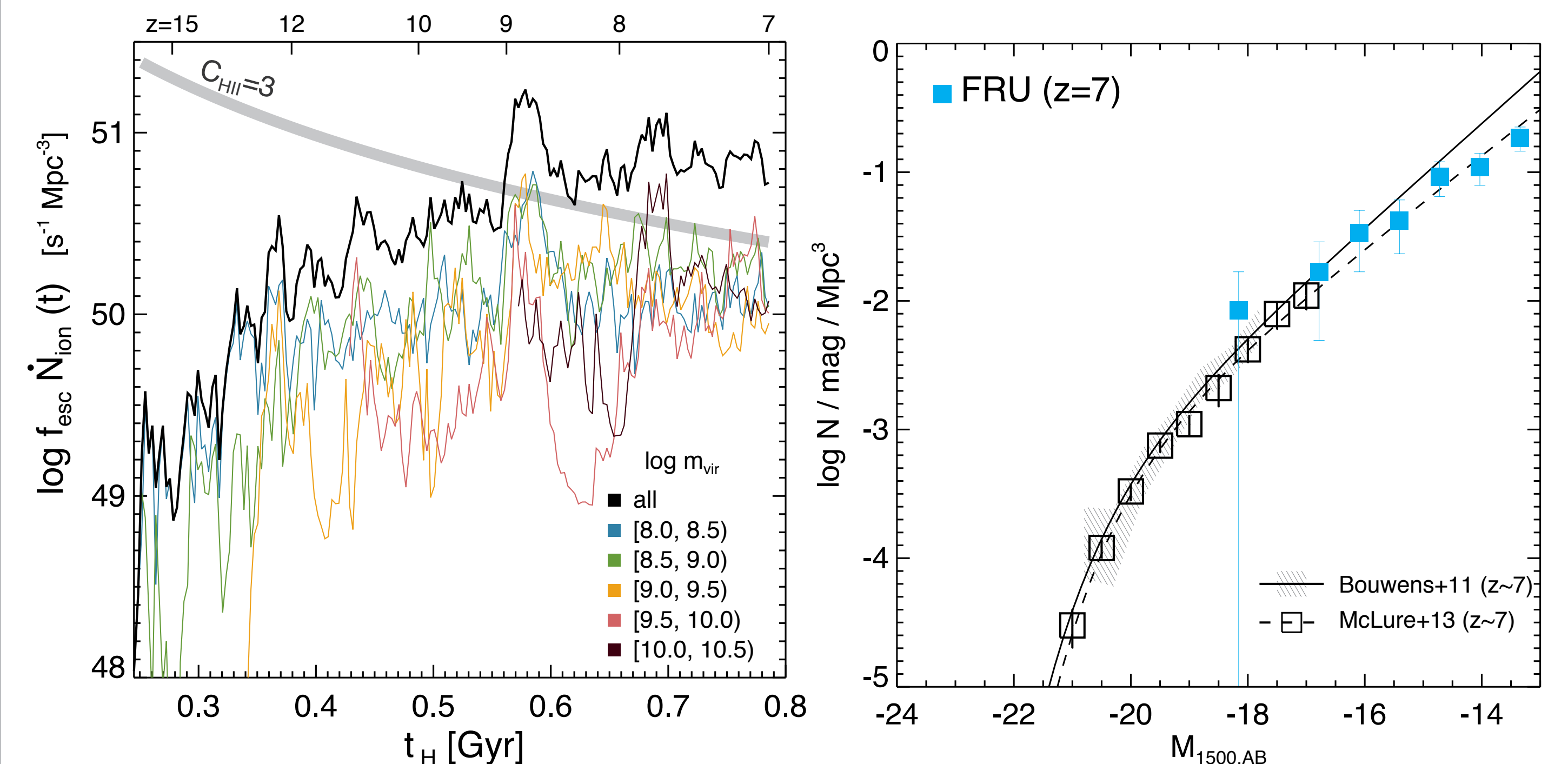


Figure 4. **Left:** Balance between the ionizing photons escaping from the dark matter halo and the recombination rate in the FRU run. The thick grey line shows the balance condition when the clumping of $C_{\text{HII}} = 3$ is used. **Right:** Rest-frame UVLF from the FRU run at $z = 7$. Observational data from Bouwens et al. (2011) and McLure et al. (2013) are shown.

Discussion

We examine whether our models provide a reasonable explanation for the reionization history. We use the Jenkins halo mass functions at different redshifts, convolved with the baryon-to-star conversion efficiency and escape fraction measured at $z=7$ from our run and Wise et al. (2014) (orange line in the middle panel of Figure 5), to derive the number of ionizing photons. Our model appears to produce enough photons to accommodate stellar reionization, although a small incremental amount of contribution by other sources (mini-halos of $M_{\text{vir}} < 10^7 M_{\text{sun}}$ or X-ray) will allow for a satisfactory account of the electron optical depth inferred by the CMB experiment (Figure 5).

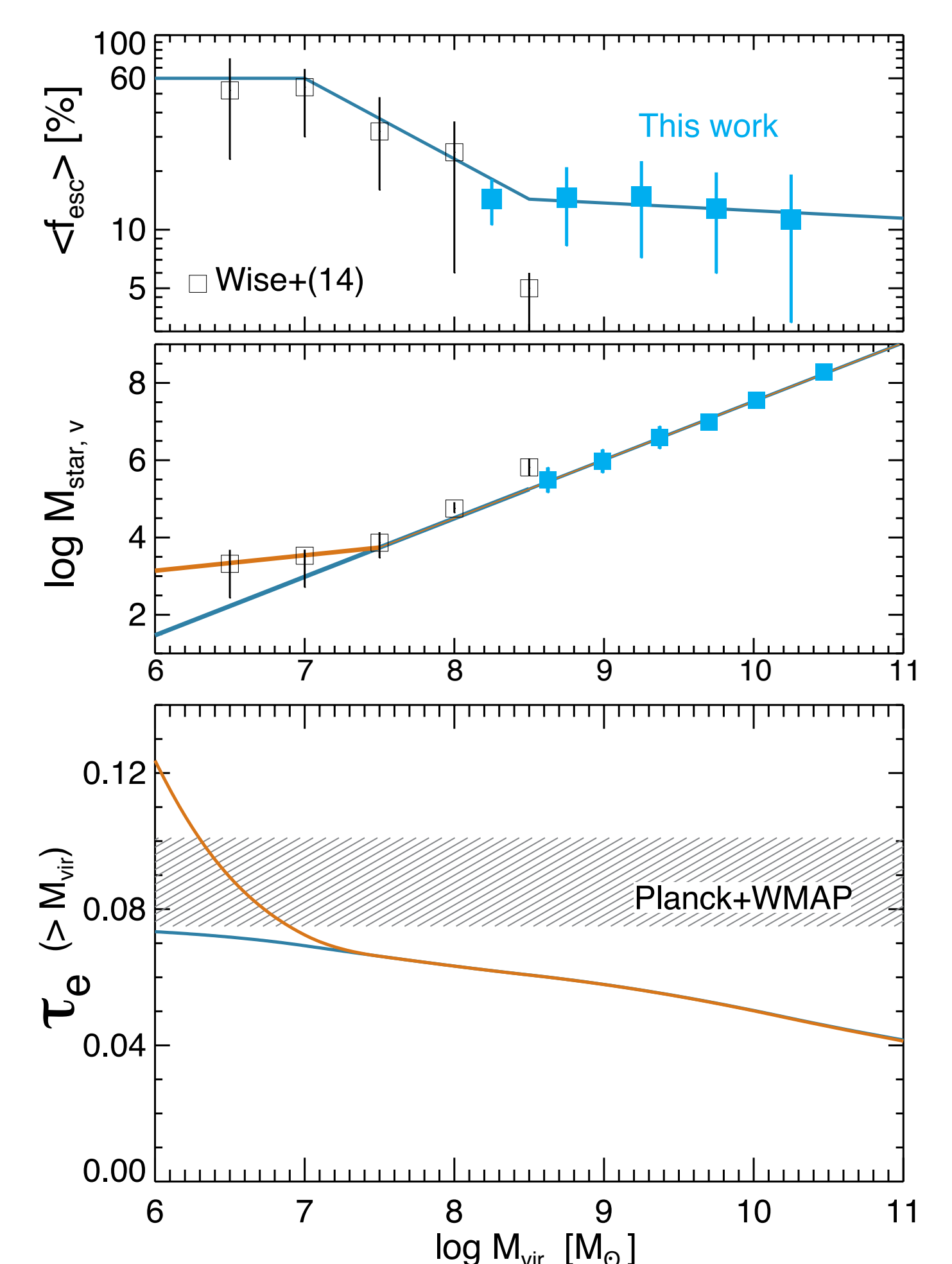


Figure 5. Semi-analytic calculations of the Thomson optical depth based on our results (blue squares) and Wise et al. (2014, black squares). The orange line shows an example of the model with an efficient baryon-to-star conversion in mini halos, as argued in Wise et al. (2014).